ChemBioChem

Chemistry Europe
European Chemical Societies Publishing
ChemBioChem

RESEARCH ARTICLE OPEN ACCESS

Charge-Based Discrimination of Amyloids Using an Amyloid-Targeting Chemiluminescent Probe

Jeewon Chung | R. Erin Jessup | Jerry Yang

Department of Chemistry and Biochemistry, University of California, San Diego, La Jolla, USA

Correspondence: Jerry Yang (jerryyang@ucsd.edu)

Received: 9 February 2026 | **Accepted:** 13 February 2026

Keywords: amyloid beta-peptides | chemiluminescence | imaging agents

ABSTRACT

Fluorescent probes have been widely developed for detecting amyloid biomarkers associated with neurodegenerative diseases (NDs). The requirement for external light for excitation, however, limits their utility for research and in vivo applications. Chemiluminescent probes, which use chemical reactions to generate emissive excited states rather than externally applied light, may offer a promising alternative to overcome some limitations for optical imaging of amyloid biomarkers. Here, we designed and synthesized a chemiluminescent amyloid-binding probe (CLIP-1) and evaluated its capability to label three amyloid biomarkers for NDs—amyloid β (Aβ), α-synuclein (α-syn), and tau protein aggregates. We found that CLIP-1 exhibits markedly enhanced chemiluminescence (CL) in aqueous solution when activated by ambient oxygen in the presence of aggregated Aβ, whereas little to no emission is observed in the absence of aggregates or in the presence of monomeric Aβ. Additionally, CLIP-1 displayed a different wavelength of emission when bound to tau aggregates compared to Aβ or α-syn aggregates, which we attribute to differences in the relative overall charge of the amyloids at neutral pH. Imaging of brain slices confirmed enhanced CL of CLIP-1 in an Alzheimer's disease mouse model, highlighting the potential for amyloid-targeting chemiluminescent probes as new tools for aiding in diagnosis of amyloid-associated neurodegenerative diseases.

1 | Introduction

Neurodegenerative diseases (NDs) such as Alzheimer's disease (AD) and Parkinson's disease (PD) represent a major public health concern due to their increasing prevalence and high mortality rates [1]. AD is primarily characterized by the abnormal accumulation of amyloid-β (Aβ) aggregates and tau neurofibrillary tangles (NFTs), while PD is associated with the aggregation of misfolded α-synuclein protein (α-syn) [2]. These pathological protein aggregates often exhibit cross β-sheet structures, a shared feature that has guided the development of various organic fluorescent probes aimed at early detection and monitoring of NDs [3, 4]. Compared to conventional clinical imaging techniques such as positron emission tomography (PET) and magnetic resonance Imaging (MRI), fluorescent probes offer advantages including high sensitivity and real-time imaging capabilities, making them suitable for early-stage detection of amyloid deposits in living patients [5, 6]. Additionally, we have previously reported a series of polarity-sensitive fluorescent probes capable of distinguishing between different types of protein aggregates based on their emission wavelengths [7], making it possible to discriminate amyloid deposits associated with different NDs.

While the potential for fluorescence-based detection of amyloids has attracted increased attention, one limitation of fluorescence is the requirement for external light excitation, which can introduce potential safety concerns in living patients and artifacts for deep-tissue imaging [8]. To overcome these challenges, researchers have begun to explore optical imaging platforms that do not require external light irradiation with the use of photoacoustic and chemiluminescent probes [9, 10]. In particular, chemiluminescent probes, which generate an emissive excited state through a chemical reaction rather than through external photon excitation, offer the potential for deeper tissue imaging and reduced

background signal [11]. In this study, we report the development and characterization of a chemiluminescent probe (CLIP-1) that is capable of targeting amyloid aggregates comprised of different protein compositions. While previous studies have explored chemiluminescent probes for detecting Aβ aggregates [12, 13], we examine the capability of a chemiluminescent probe to detect three different amyloids and show, for the first time, that a chemiluminescent probe can exhibit different wavelengths of emission depending on the expected relative charge along the amyloid surface. This work advances the field by going beyond simple detection of amyloids as we investigate how charge as a microenvironmental factor associated with different types of amyloid aggregates can influence the chemiluminescence (CL) profile of the probe.

2 | Results and Discussion

Imidazo[1,2-a]pyrazin-3(7H)-one (IPO, Figure 1A) is an oxygen-driven chemiluminescent scaffold, which has been used for detection of reactive oxygen species (ROS) such as superoxide anion [14, 15]. Many groups have attempted to develop chemiluminescent probes comprising an IPO moiety that can target specific biomarkers. For instance, the Ran group recently reported the ADLumin series (Figure 1B) of chemiluminescent probes that incorporates an IPO moiety and was able to show CL activation in the presence of Aβ aggregates [12, 13]. Here, we hypothesized that incorporation of an IPO moiety into an amyloid-targeting scaffold with known environmental sensitivity and spectroscopic properties could offer additional advantages for amyloid imaging. Figure 1C depicts the chemical structure of ARCAM-1, an environmentally sensitive fluorescent amyloid-targeting probe that we showed could discriminate amyloids based on differences in binding pocket polarities [7] and whose spectroscopic properties could be tuned through chemical modifications on the scaffold [4]. We designed CLIP-1 with the hypothesis that incorporation of an IPO moiety on the aminonaphthalene scaffold of ARCAM-1 would retain the amyloid binding and some spectroscopic properties of ARCAM-1, but could generate light through a known CL pathway (Figure 1D). Details for the synthesis and characterization of CLIP-1 are provided in the supporting information.

We first confirmed that CLIP-1 could bind to aggregated Aβ using a previously reported assay [16], which revealed a K_d of 5.6 μM (Figure S1) that was similar to the binding of ARCAM-1 to aggregated Aβ (6.3 μM) [4]. Figure 2A shows the CL of CLIP-1 increased in the presence of increasing concentrations of aggregated Aβ in solution after a 5 min incubation time. Remarkably, we observe no CL in aqueous solution in the absence of aggregated Aβ and relatively little CL from CLIP-1 with increasing concentrations of nonaggregated Aβ in the same measurement time window (Figure 2B). Prior studies on IPO-related CL have shown that molecular oxygen is required to initiate the oxidation process leading to light emission [17, 18]. We, therefore, measured the CL spectrum of CLIP-1 in the presence of Aβ aggregates with and without bubbling of oxygen (Figure 2C). We observed an approximate 2-fold increase in intensity of CL from CLIP-1 in the presence of oxygen bubbling, which is consistent with an oxygen-dependent mechanism for CL activation. LC–MS analysis also confirmed that CLIP-1 converted to the expected products (Figure 1D) after reaction with oxygen in the presence of aggregated Aβ, showing 77% substrate conversion and 28% yield of oxidation products (Figure S2).

To help understand the mechanism for CL enhancement of CLIP-1 in the presence of Aβ, we first examined whether CLIP-1 undergoes oxidation under ambient oxgyen in the absence of Aβ if incubated for a long period of time. LC–MS spectra acquired before and after 24 h incubation of CLIP-1 in nanopure water revealed new peaks corresponding to oxidized species, indicating that CLIP-1 can oxidize—albeit very slowly—even without Aβ (Figure S3). We next evaluated the oxidation kinetics by monitoring the time-dependent CL in the presence and absence of Aβ aggregates (Figure S4). The observed rate constant (k_{obs}) increased ≈30-fold with Aβ aggregates, from 0.01 min^{-1} in the absence of Aβ to 0.31 min^{-1} in the presence of Aβ aggregates, demonstrating that Aβ aggregates markedly accelerate CLIP-1 oxidation. The combined LC–MS and kinetic results together suggest that CLIP-1 does oxidize in the absence of Aβ, but the rate is extremely slow, resulting in only weak CL observable after 24 h incubation. Aβ accelerates the oxidation process, leading to substantially higher

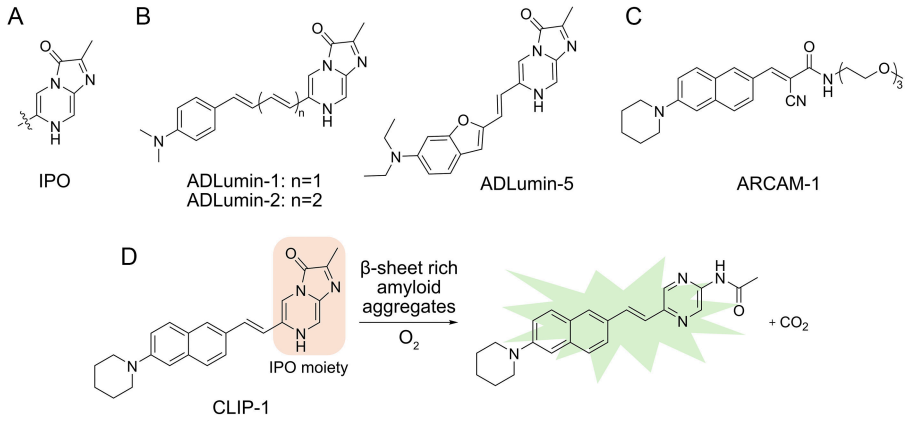

FIGURE 1 | Structure of (A) Imidazo[1,2-a]pyrazin-3(7H)-one (IPO) moiety, (B) a previously reported class of Aβ-targeting IPO-based chemiluminescent probes (ADLumin series) [12, 13], and (C) an environmentally sensitive amyloid-targeting fluorescent probe, ARCAM-1 [7]. (D) Schematic illustration of CLIP-1 generating chemiluminescence upon activation with oxygen.

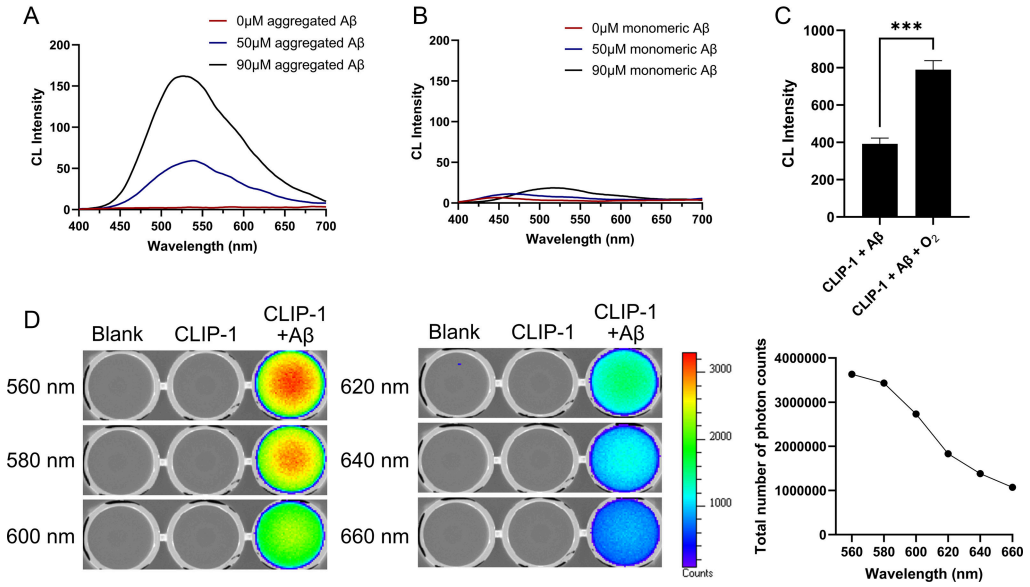

FIGURE 2 | Spectroscopic properties of CLIP-1. Chemiluminescence (CL) spectra of CLIP-1 in solution with increasing concentrations of aggregated (A) or monomeric (B) Aβ. (C) Chemiluminescence intensity of CLIP-1 with Aβ aggregates without or with oxygen bubbling (30 min). *** represents a p value of 0.0003 using Student's t-test ($n = 3$). (D) Chemiluminescence images and quantitative plot of photon counts of aqueous solutions of CLIP-1 acquired at different emission wavelengths using an IVIS system.

chemiluminescent signal intensity that is observable even after only a 5 min incubation. The CL quantum yield of CLIP-1 was calculated to be 0.195% (1.95×10^{-3} einsteins/mol) in the presence of Aβ aggregates and 0.0216% (2.16×10^{-4} einsteins/mol) in the absence of Aβ aggregates using luminol as standard according to published protocol [12, 19].

CL imaging of CLIP-1 using an in vivo imaging system (IVIS) with and without Aβ aggregates is shown in Figure 2D. Again, no detectable signal from CLIP-1 was observed in the absence of amyloid, while strong CL was detected in samples containing aggregated Aβ. Total photon counts at 6 different wavelengths were quantified from the acquired images using all available filters for the IVIS system and showed the highest number of photon counts for CLIP-1 at 560 nm.

In order to examine whether CLIP-1 could detect amyloid aggregates derived from proteins other than Aβ, we prepared solutions of recombinant α-synuclein (α-syn) and tau protein according to previously reported protocols [20, 21]. We measured binding constants (K_d) of 1.7 μM and 2.8 μM for CLIP-1 to aggregated α-syn and tau, respectively, which were similar to the binding of this probe to aggregated Aβ (SI Figures S5 and S6). We also observed an increase in CL of CLIP-1 in the presence of aggregated α-syn and tau as we had observed in the presence of aggregated Aβ in aqueous buffer at pH 7.2. However, the CL spectra indicated a ~30 nm difference in emission wavelength maximum for CLIP-1 in the presence of tau protein aggregates relative to the presence of Aβ or α-syn aggregates (Figure 3 and Figure S7). As the emission maximum (λ_{max}) serves as a robust metric for colorimetric discrimination commonly used to discriminate distinct protein compositions [22, 23], we focused our analysis on this wavelength shift.

To investigate a potential reason for the difference in emission maximum for CLIP-1 in the presence of tau compared to Aβ and α-syn, we first measured the CL of CLIP-1 in various polar aprotic organic solvents with different solvent polarity. In contrast to the strong dependence of fluorescence emission wavelength of ARCAM-1 on environmental polarity [24], we did not observe any obvious trend in intensity or wavelength of CL emission for CLIP-1 as a function of solvent polarity (Figure S8).

Previous studies on IPO-containing chemiluminescent molecules showed that oxidation can generate two different emissive excited states, one that is negatively charged and one that is electrically neutral (Figure 4A) [12, 17, 25, 26]. Based on the results shown in Figure 3 and the reported pIs of Aβ (5.3) [27], α-syn (4.7) [28], and tau (8.2) [29], we hypothesize that the overall charge of the amyloids at pH 7.2 would be negative for Aβ and α-syn aggregates, but positive for tau aggregates. These differences in overall charge of the amyloid could, in turn, favor the formation of the anionic excited state when bound to tau aggregates (leading to longer wavelength emission) and disfavor the anionic excited state (and, thus, favor the neutral excited state with shorter wavelength emission) when bound to Aβ and α-syn aggregates. To test this hypothesis, we examined the pH dependence of CL of CLIP-1 in

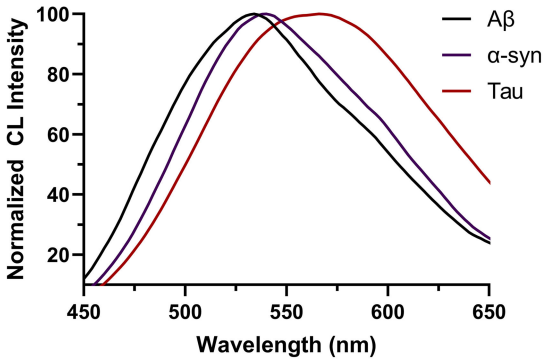

FIGURE 3 | Normalized chemiluminescence spectra of CLIP-1 (10 μM) in the presence of 50 μM Aβ, α-syn, and tau aggregates at pH 7.2. The observed emission maxima (λ_{max}) were 534, 540, and 566 nm for Aβ, α-syn, and tau, respectively.

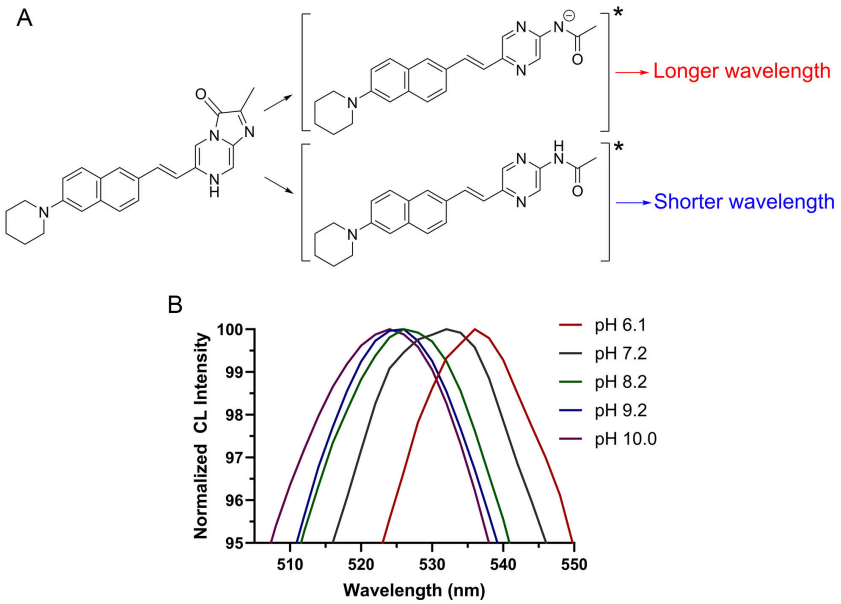

FIGURE 4 | (A) Schematic illustration of CLIP-1 having two different emissive excited states responsible for chemiluminescence emission as proposed in prior studies [12]. (B) Normalized chemiluminescence spectra of CLIP-1 in the presence of aggregated Aβ at different pHs.

the presence of Aβ aggregates (Figure 4B) and found a trend of increasing wavelengths of emission with decreasing pH. Here, we examined CL of CLIP-1 at pHs between 6.1 and 10.0, as solutions below pH 6.1 resulted in significant loss of signal possibly due to nonradiative pathways that have also been reported for chemiluminescent IPO compounds in acidic solutions [30]. We also performed a similar experiment as shown in Figure 3, but suggest that CLIP-1 may function as an environmentally sensitive chemiluminescent probe, with emission properties modulated by the local charge on different amyloid aggregates.

Finally, to further evaluate CLIP-1 for the capability to detect amyloid deposits in brain, we first confirmed that neuronal tissue sections from an AD mouse model (APP-SAA KI) contained strongly fluorescent Aβ plaques when stained with ARCAM-1, whereas control brain slices did not contain any detectable amyloid deposits. We then incubated tissue slices obtained from the same mouse brains with CLIP-1 and imaged them using the IVIS system without external photon excitation (Figure 5B). Figure 5C shows a nearly 2-fold increase in signal for the AD versus the control brain, indicating enhanced CL intensity of the probe in the presence of endogenous Aβ aggregates in tissue. These results indicate that amyloid binding is essential for achieving enhanced CL in tissue, enabling detection over any background nonspecific signals present in biological samples.

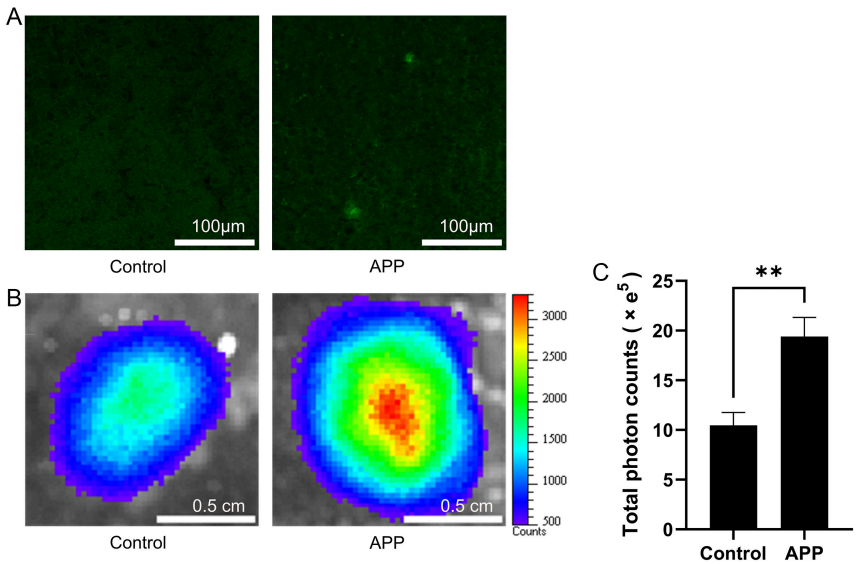

FIGURE 5 | (A) Confocal fluorescence microscopic images of tissue slices from control and AD brain (APP) stained with ARCAM-1. (B) Ex vivo chemiluminescence images of neuronal tissue slices acquired using the IVIS system after incubation with CLIP-1. (C) Average total photon counts extracted from the obtained chemiluminescence images. ** represents a p value of 0.0025 using Student's t-test ($n = 3$).

3 | Conclusion

In conclusion, we developed a new probe, CLIP-1, that shows enhanced CL emission when bound to amyloid aggregates associated with different neurodegenerative diseases. The design of CLIP-1 incorporates structural features of ARCAM-1, known to promote amyloid binding and exhibit an environmentally dependent colorimetric response. It showed different CL emission profiles when bound to tau aggregates compared to aggregates of Aβ and α-syn, which we attribute to differences in the local charge of the amyloids at neutral pH. Furthermore, tissue imaging with CLIP-1 showed enhanced CL in the presence of amyloid deposits, demonstrating the potential for using this probe for detecting amyloidosis in neuronal samples without the need for an external light source. These findings establish a new mechanistic foundation for discrimination of amyloids associated with different NDs using CL.

Acknowledgments

This work was supported by the National Institute on Aging of the National Institutes of Health under award numbers 1RF1AG077802-01 and 4R01AG077802-02. We thank Professor Christina Sigurdson for generously providing tissue samples. We also appreciate Dr. Meihan Li and Dr. Lannah Abasi for their kind donation of α-synuclein and tau proteins. We thank Prof. Chongzhao Ran with helpful advice for the final step in the synthesis of CLIP-1. We are grateful to Dr. Yongxuan Su at the UCSD Mass Spectrometry Facility for assistance with mass spectrometric analysis. Confocal microscopy imaging was performed at the UCSD SOM Microscopy Core (NS047101, OD030505, and OD036455). Also, we thank Dr. Kersi Pestonjamasp at UCSD Cancer Center Microscopy Shared Facility and the Specialized Support Grant (P30 CA23100-28).

Conflicts of Interest

J.Y. is a founder and equity interest holder in Amydis, Inc. All other authors declare no conflicts of interest.

Data Availability Statement

The data that support the findings of this study are available in the supplementary material of this article.

References

1. Alzheimer's Association, "2024 Alzheimer's Disease Facts and Figures," *Alzheimer's & Dementia* 20 (2024): 3708–3821.

2. C. A. Ross and M. A. Poirier, "Protein Aggregation and Neurodegenerative Disease," *Nature Medicine* 10, no. S7 (2004): S10–S17.

3. J. Zhou, P. Jangili, S. Son, M. S. Ji, M. Won, and J. S. Kim, "Fluorescent Diagnostic Probes in Neurodegenerative Diseases," *Advanced Materials* 32 (2020): 2001945.

4. R. S. Ehrlich, A. L. Shiao, M. Li, et al., "Exploring the Effect of Aliphatic Substituents on Aryl Cyano Amides on Enhancement of Fluorescence upon Binding to Amyloid-β Aggregates," *ACS Chemical Neuroscience* 12 (2021): 2946–2952.

5. C. Kerbage, C. H. Sadowsky, D. Jennings, G. D. Cagle, and P. D. Hartung, "Alzheimer's Disease Diagnosis by Detecting Exogenous Fluorescent Signal of Ligand Bound to Beta Amyloid in the Lens of the Human Eye: An Exploratory Study," *Frontiers in Neurology* 4 (2013): 62.

6. C. Kerbage, C. H. Sadowsky, P. N. Tariot, et al., "Detection of Amyloid β Signature in the Lens and Its Correlation in the Brain to Aid in the Diagnosis of Alzheimer's Disease," *American Journal of Alzheimer's Disease & Other Dementias* 30 (2015): 738–745.

7. K. J. Cao, K. M. Elbel, J. L. Cifelli, et al., "Solvation-Guided Design of Fluorescent Probes for Discrimination of Amyloids," *Scientific Reports* 8 (2018): 6950.

8. V. Ntziachristos, J. Ripoll, L. V. Wang, and R. Weissleder, "Looking and Listening to Light: The Evolution of Whole-Body Photonic Imaging," *Nature Biotechnology* 23 (2005): 313–320.

9. J. Huang and K. Pu, "Activatable Molecular Probes for Second Near-Infrared Fluorescence, Chemiluminescence, and Photoacoustic Imaging," *Angewandte Chemie International Edition* 59 (2020): 11717–11731.

10. M. Yang, J. Huang, J. Fan, J. Du, K. Pu, and X. Peng, "Chemiluminescence for Bioimaging and Therapeutics: Recent Advances and Challenges," *Chemical Society Reviews* 49 (2020): 6800–6815.

11. Y. Yang and F. Zhang, "Activatable Chemiluminescent Molecular Probes for Bioimaging and Biosensing," *Analysis & Sensing* 1 (2021): 75–89.

12. J. Zhang, C. Wickizer, W. Ding, et al., "In Vivo Three-Dimensional Brain Imaging with Chemiluminescence Probes in Alzheimer's Disease Models," *Proceedings of the National Academy of Sciences of the United States of America* 120, no. 50 (2023): e2310131120.

13. J. Yang, W. Yin, R. Van, et al., "Turn-On Chemiluminescence Probes and Dual-Amplification of Signal for Detection of Amyloid Beta Species In Vivo," *Nature Communications* 11 (2020): 1–14.

14. K. Teranishi, "Development of Imidazopyrazinone Red Chemiluminescent Probes for Detecting Superoxide Anions via a Chemiluminescence Resonance Energy Transfer Method," *Luminescence: the Journal of Biological and Chemical Luminescence* 22 (2007): 147–156.

15. K. Teranishi and O. Shimomura, "Coelenterazine Analogs as Chemiluminescent Probes for Superoxide Anion," *Analytical Biochemistry* 249 (1997): 37–43.

16. Y. Guan, K. J. Cao, A. Cantlon, et al., "Real-Time Monitoring of Alzheimer's-Related Amyloid Aggregation via Probe Enhancement–Fluorescence Correlation Spectroscopy," *ACS Chemical Neuroscience* 6 (2015): 1503–1508.

17. K. Teranishi, "Luminescence of Imidazo[1,2-a]pyrazin-3(7H)-One Compounds," *Bioorganic Chemistry* 35 (2007): 82–111.

18. I. M. Mostafa, A. Abdussalam, Y. T. Zholudov, et al., "Recent Applications and Future Perspectives of Chemiluminescent and Bioluminescent Imaging Technologies," *Chemical & Biomedical Imaging* 1 (2023): 297–314.

19. X. Zhen, C. Zhang, C. Xie, Q. Miao, K. L. Lim, and K. Pu, "Intraparticle Energy Level Alignment of Semiconducting Polymer Nanoparticles to Amplify Chemiluminescence for Ultrasensitive In Vivo Imaging of Reactive Oxygen Species," *ACS Nano* 10 (2016): 6400–6409.

20. J. L. Cifelli, C. C. Capule, and J. Yang, "Noncovalent, Electrostatic Interactions Induce Positively Cooperative Binding of Small Molecules to Alzheimer's and Parkinson's Disease–Related Amyloids," *ACS Chemical Neuroscience* 10 (2019): 991–995.

21. A. J. Dregni, V. S. Mandala, H. Wu, et al., "In Vitro 0N4R Tau Fibrils Contain a Monomorphic β-Sheet Core Enclosed by Dynamically Heterogeneous Fuzzy Coat Segments," in *Proceedings of the National Academy of Sciences of the United States of America*, (2019), 16357–16366, 116

22. E. C. Carroll, H. Yang, W. C. Powell, et al., "High-Throughput Discovery of Fluoroprobes That Recognize Amyloid Fibril Polymorphs," *Nature Chemistry* 17 (2025): 1565–1575.

23. T. Klingstedt, A. Åslund, R. A. Simon, et al., "Synthesis of a Library of Oligothiophenes and Their Utilization as Fluorescent Ligands for Spectral Assignment of Protein Aggregates," *Organic & Biomolecular Chemistry* 9 (2011): 8356–8370.

24. W. M. Chang, M. Dakanali, C. C. Capule, C. J. Sigurdson, J. Yang, and E. A. Theodorakis, "ANCA: A Family of Fluorescent Probes That Bind and

Stain Amyloid Plaques in Human Tissue," *ACS Chemical Neuroscience* 2 (2011): 249–255.

25. Y. Kambayashi and K. Ogino, "Reestimation of Cypridina Luciferin Analogs (MCLA) as a Chemiluminescence Probe to Detect Active Oxygen Species," *Journal of Toxicological Sciences* 28, no. 3 (2003): 139–148.

26. K. Teranishi, M. Hisamatsu, and T. Yamada, "Studies on the Mechanism of Chemiluminescence: Synthesis and Chemiluminescent Properties of the 5-Hydroperoxide Analogue of Coelenterate Luciferin," *Journal of Biochemistry* 120 (1996): 118–125.

27. Y. Tian and J. H. Viles, "PH Dependence of Amyloid-β Fibril Assembly Kinetics: Unravelling the Microscopic Molecular Processes," *Angewandte Chemie International Edition* 61 (2022): e202210675.

28. K. Furukawa, C. Aguirre, M. So, et al., "Isoelectric Point–Amyloid Formation of α-Synuclein Extends the Generality of the Solubility- and Supersaturation-Limited Mechanism," *Current Research in Structural Biology* 2 (2020): 35–44.

29. S. Park, J. H. Lee, J. H. Jeon, and M. J. Lee, "Degradation or Aggregation: The Ramifications of Post-Translational Modifications on Tau," *BMB Reports* 51 (2018): 265.

30. K. Fujimori, S. Hiromitsu Nakajima, K. Akutsu, M. Mitani, H. Sawada, and M. Nakayama, "Chemiluminescence of Cypridina Luciferin Analogues. Part 1. Effect of pH on Rates of Spontaneous Autoxidation of CLA in Aqueous Buffer Solutions," *Bulletin of the Chemical Society of Japan* 66 (1993): 2345–2351.

Supporting Information

Additional supporting information can be found online in the Supporting Information section.